ACI STRUCTURAL JOURNAL TECHNICAL PAPER

Title no. 107-S07

Pushover Analysis of Shear-Critical Frames: Formulation

by Serhan Guner and Frank J. Vecchio

An analytical procedure is presented for the nonlinear analysis of reinforced concrete frame structures consisting of beams, columns, and shear walls under monotonic and pushover loads. The procedure is capable of accurately representing shear-related mechanisms coupled with flexural and axial behaviors. The formulation described herein uses linear-elastic frame analysis algorithms in a nonlinear mode based on an unbalanced force approach. Rigorous nonlinear sectional analyses of concrete member cross sections, using a distributed-nonlinearity fiber model, are performed based on the disturbed stress field model. The proposed method is distinct from existing methods in that it allows for the inherent and accurate consideration of shear effects and significant second-order mechanisms within a simple modeling process suitable for practical applications. Decisions regarding the anticipated behavior and failure mode or the selection of appropriate analysis options and parameter values, or additional supporting calculations such as the moment-axial force or shear force-shear deformation responses, are not required.

Keywords: beam column; fiber model; frame structure; monotonic; nonlinear analysis; pushover; reinforced concrete; retrofit; shear.

INTRODUCTION

The analysis and design procedures that have been incorporated into modern design codes typically require frame structures to be analyzed linear-elastically and designed for ductile and flexure-critical behavior. Although linear-elastic analyses cannot accurately predict all aspects of structural behavior, such as redistribution of forces and service load deformations, they are deemed sufficient if the structure is designed for flexural behavior. There are numerous analytical tools that can perform such an analysis and design reasonably well. In some situations, however, it may be necessary to analyze a shear-critical structure to more accurately predict its behavior. Such an analysis may be required for the safety assessment of existing structures that were built 20 years ago or earlier based on practices considered deficient today; damaged or deteriorated structures; accurate assessment of large, atypical, or unique structures; investigation of rational retrofit alternatives in structures requiring rehabilitation; and forensic analyses in cases of structural failure. Furthermore, modern building codes such as IBC (2006) and FEMA 356 (2000) favor more accurate procedures over traditional linear-elastic methods for a more thorough analysis.

Such analyses can be performed using nonlinear analysis procedures that typically require computer-based applications. Most available applications for this purpose, however, such as SAP2000® (CSI 2005), RUAUMOKO (Carr 2005) and DRAIN-2DX (Prakash et al. 1993), ignore shear mechanisms by default. If the structure being analyzed is in fact shear-critical, severely unconservative estimates of both strength and ductility are typically obtained. Unlike flexure-critical structures, shear-critical structures fail in a much less forgiving, brittle manner with little or no forewarning; therefore, consideration of shear behavior is essential for safe and realistic assessment of structural performance.

Some available computer tools for frame structures, such as SAP2000, permit the consideration of shear behavior through automatically generated shear hinges based on simple formulas; however, there is typically insufficient information available on the applicability of these formulas to the frame being analyzed. As a result, grossly inaccurate results for both strength and ductility predictions are commonly obtained when using such generic or unknown models for the shear behavior. On the other hand, some available tools, such as RUAUMOKO, permit the analyst to define the shear behavior manually through user-defined shear hinges. Creation of this input, however, requires expert knowledge on the shear behavior of concrete and usually takes significant time and effort even when using other computer programs for the shear calculations, which severely limits the use of such procedures in practice. In addition, whether considering shear behavior or not, the analyst is typically required to select from a list of models and options appropriate for the frame being analyzed. These may include material models, such as the concrete tensile or compressive response models, or nonlinear analysis options, such as large displacements or hinge unloading methods. The selection of these options tends to have a significant effect on the computed response and may render the analytical results questionable if not properly selected. This further limits the use of existing tools by practicing structural engineers.

Consider, for example, a frame specimen tested by Duong et al. (2007) involving a one-bay, two-story, shear-critical frame. The frame was tested under a monotonically increasing lateral load applied to the second-story beam and two constant column loads applied to simulate the axial force effects of higher stories. For analysis purposes, two software programs were used: SAP2000 and RUAUMOKO. Both analyses were performed with the use of only default options and models. For modeling the hinges, the default moment and shear hinges were used in the SAP2000 model, and the default moment hinges, the only available option, were used in the RUAUMOKO model. As seen in Fig. 1, highly contradictory and inaccurate predictions were obtained for both strength and ductility. SAP2000 underestimated the strength by 70%, predicting a shear failure; RUAUMOKO overestimated it by 25%, predicting a flexural failure. The RUAUMOKO analysis did not provide any indication of the ultimate displacement; the analysis carried on sustaining the ultimate load based on the elastic-plastic hinge behavior. SAP2000,

ACI Structural Journal, V. 107, No. 1, January-February 2010.
MS No. S-2008-381 received November 23, 2008, and reviewed under Institute publication policies. Pertinent discussion including author's closure, if any, will be published in the November-December 2010 *ACI Structural Journal* if the discussion is received by July 1, 2010.

ACI member **Serhan Guner** *is a Structural Designer at Morrison Hershfield Limited, Toronto, ON, Canada. He received his PhD in 2008 from the University of Toronto, Toronto, ON, Canada. His research interests include nonlinear analysis and performance assessment of reinforced concrete structures, shear effects in reinforced concrete, and structural dynamics and seismic response.*

Frank J. Vecchio, *FACI, is a Professor of civil engineering at the University of Toronto. He is a member of Joint ACI-ASCE Committees 441, Reinforced Concrete Columns, and 447, Finite Element Analysis of Concrete Structures. He received the 1998 ACI Structural Research Award and the 1999 ACI Structural Engineering Award. His research interests include advanced constitutive modeling and analysis of reinforced concrete, assessment and rehabilitation of structures, and response under extreme load conditions.*

on the other hand, predicted an erroneous 4.0 mm (0.16 in.) failure displacement. The actual failure displacement in the test was expected to be only slightly more than the 44.8 mm (1.76 in.) attained (Duong et al. 2007). More details of these analyses are provided by Guner (2008).

This current study is concerned with the development and verification of an analytical method for the nonlinear analysis of frame-related structures with particular emphasis on shear-related mechanisms. A frame analysis program, VecTor5, based on predecessor program TEMPEST (Vecchio 1987; Vecchio and Collins 1988), was developed for accurate simulations under monotonic and pushover loading conditions. The procedure is distinct from others in its inherent and accurate consideration of shear effects and significant second-order mechanisms within a simple modeling process suitable for use by practicing structural engineers. Decisions regarding the expected behavior and failure mode or selection of appropriate values for multiple parameters and options are not required prior to the analyses, nor are additional supporting calculations such as moment-axial force, moment-curvature, or shear force-shear deformation responses of the cross sections.

RESEARCH SIGNIFICANCE

Although modern design codes typically require frame structures to be designed for ductile behavior, situations often arise in practice where shear-related mechanisms play a significant role. Currently available analytical tools either ignore shear mechanisms altogether, employ unclear or overly simplistic formulations, or are overly complex, requiring the selection of numerous analysis options and input of supporting calculations prior to the analysis. Most neglect shear deformations by default. Thus, improved analytical tools are much needed. This study describes a nonlinear analysis procedure for plane frames that provides a comprehensive and accurate assessment of shear effects—one that does not require precalculation of interaction responses or failure modes, nor the selection of a confusing array of analysis options and material models.

OVERVIEW OF PROPOSED ANALYTICAL PROCEDURE

The analytical procedure proposed is based on a total load, iterative, secant stiffness formulation. The computer-based calculation procedure consists of two interrelated analyses. First, a linear-elastic global frame analysis, using a classical stiffness-based finite element formulation, is performed to obtain member deformations. Using the calculated deformations, nonlinear sectional analyses are performed to determine the sectional member forces, based on a distributed-nonlinearity fiber approach. The differences between the global and sectional forces are termed the

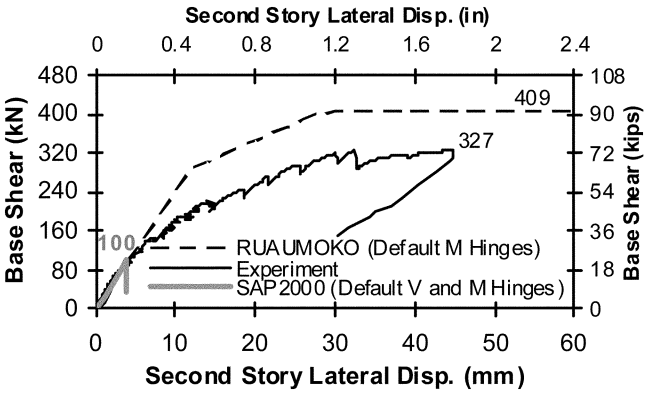

Fig. 1—Comparison of load-deflection responses for Duong et al. (2007) frame.

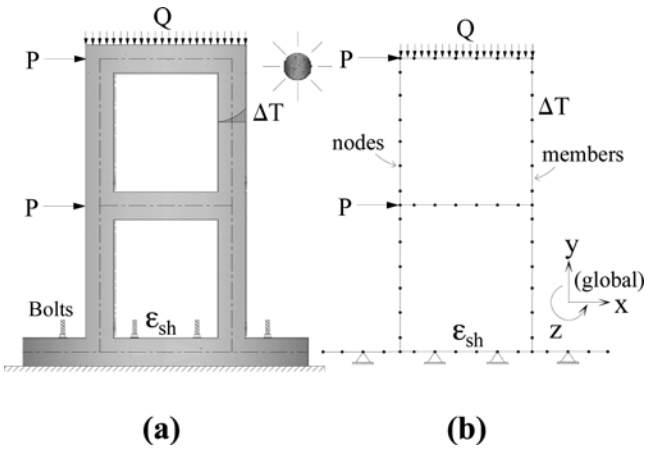

Fig. 2—Creation of global frame model: (a) structure and loading; and (b) global frame model.

"unbalanced forces," which are added to the "compatibility restoring forces" (that is, virtual static loads) to force member deformations in the global frame analysis to match those in the nonlinear sectional analysis. The compatibility restoring forces are applied to the ends of each member in a self-equilibrating manner. The global frame analysis and the sectional analyses are performed iteratively, resulting in a double-iterative procedure, until all unbalanced forces converge to zero. In all calculations, the initial transformed cross-sectional area A_t and moment of inertia I_t are used together with the initial tangent Young's modulus of concrete E_t. The procedure allows the analysis of frames with unusual or complex cross sections under a wide range of static and thermal load conditions. Nonlinear thermal analysis calculations were adopted from the predecessor procedure TEMPEST.

To analyze a structure with the proposed analytical procedure, a global model of the structure must first be created by dividing frame elements (that is, beams, columns, and shear walls) into a number of members (that is, segments). All mechanical and thermal forces acting on the structure, as well as support conditions, must be defined as shown in Fig. 2. Unlike lumped-nonlinearity frame elements with plastic hinges located at each end, the frame element proposed is based on a distributed-nonlinearity fiber model where nonlinear behavior is monitored at each member using average member forces. Therefore, reasonably short members should be used in the model to adequately capture

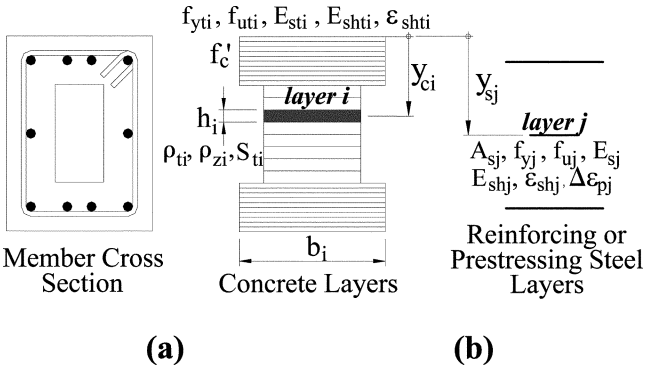

Fig. 3—Creation of sectional model: (a) cross section; and (b) sectional model.

the nonlinear behavior. For optimal accuracy, the recommended member length is in the range of 50% of the cross section depth for beam and column members and 10% of the cross section depth for shear wall members. A more detailed description of the modeling and analysis process is provided by Guner and Vecchio (2008) and Guner (2008).

A layered (fiber) analysis technique is employed for the nonlinear sectional analyses; therefore, a sectional model of each cross section used in the frame model must be created by dividing the cross section into a number of concrete layers, longitudinal reinforcing bar layers, and longitudinal prestressing steel layers. A sectional model and the material properties required for the input are shown in Fig. 3, where f_c' is the concrete compressive strength; ρ_{ti} and ρ_{zi} are the transverse and out-of-plane reinforcement ratios, respectively; S_{ti} is the spacing of the transverse reinforcement in the longitudinal direction; f_{yti} and f_{uti} are the yield and ultimate stresses of the transverse reinforcement, respectively; E_{sti} and E_{shti} are the Young's and the strain hardening moduli of the transverse reinforcement, respectively; ε_{shti} is the strain at the onset of strain hardening; A_{sj} is the total cross-sectional area of the longitudinal reinforcement or prestressing steel layer; and $\Delta\varepsilon_{pj}$ is the locked-in strain differential for the prestressing steel layer.

At the end of the analysis, the procedure provides sufficient output to fully describe the behavior of the structure, including the load-deflection response, member deformations and deflections, concrete crack widths, reinforcement stresses and strains, deficient parts and members (if any), and failure mode and failure displacement of the structure. The postpeak response of the structure is also provided, through which the energy dissipation and the displacement ductility can be calculated.

BASIC ANALYSIS STEPS

1. The procedure starts with adding current compatibility restoring forces to the fixed-end forces due to applied mechanical loads. In the first iteration of the first load stage, the compatibility restoring forces are taken as zero.

2. A linear-elastic frame analysis of the structure is performed to determine the joint displacements, joint reactions, and member end-actions. Using appropriate end factors, the average internal forces of each member (that is, N_k, M_k, and V_k) are determined. The geometry of the structure is updated based on the joint displacements computed.

3. The axial and shear strain distributions through the depth of each member are determined.

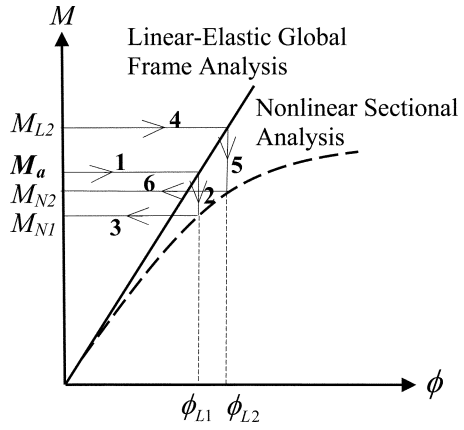

Fig. 4—Unbalanced force approach.

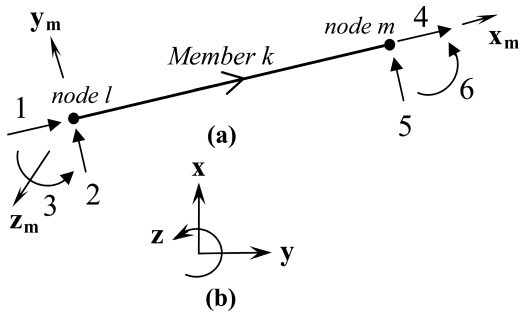

Fig. 5—Frame member: (a) degrees-of-freedom in member-oriented axes; and (b) global axes.

4. Nonlinear sectional analysis iterations are performed for each member to calculate the sectional forces, that is, $N_{sec\,k}$, $M_{sec\,k}$, and $V_{sec\,k}$.

5. The unbalanced forces (that is, the differences between the global and sectional forces) are calculated for each member. These unbalanced forces are added to the compatibility restoring forces to be applied to the structure.

6. The aforementioned calculations are repeated until all unbalanced forces become zero or the maximum number of iterations is reached.

To illustrate the concept of unbalanced forces, the response of a member to an applied moment M_a in the first two iterations is shown in Fig. 4. For M_a and curvature ϕ_{L1}, calculated from the linear-elastic global frame analysis, nonlinear sectional moment is calculated as M_{N1} in the first iteration (arrows 1 to 3 in Fig. 4). The difference between M_a and M_{N1} is the unbalanced moment M_{U1}, which is added to the compatibility restoring force ($M_{R1} = 0 + M_{U1}$) to be applied to the member as $M_{L2} = M_a + M_{R1}$ to find M_{N2}. Notice how the unbalanced moment ($M_{U2} = M_a - M_{N2}$) reduces while the compatibility restoring force ($M_{R2} = M_{U1} + M_{U2}$) increase. The procedure is continued in this manner until M_N becomes equal to M_a.

LINEAR-ELASTIC GLOBAL FRAME ANALYSIS

A typical frame member is shown in Fig. 5, relative to the member-oriented local coordinate system axes x_m, y_m, and z_m. A flowchart indicating the major steps in the global frame analysis procedure is presented in Fig. 6.

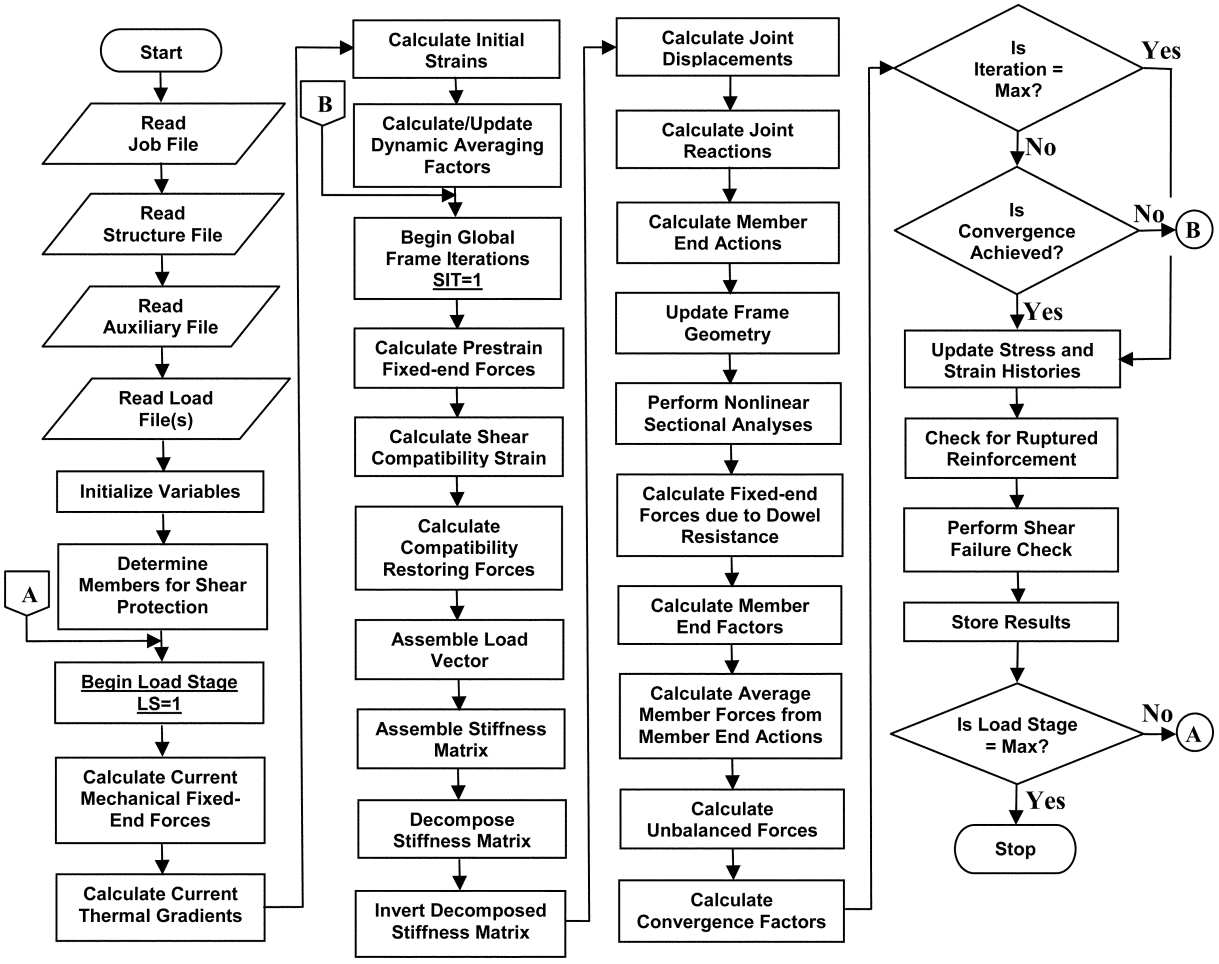

Fig. 6—Flowchart for global frame analysis.

Shear protection algorithm

In the analysis of frames that are typically modeled accordingly to centerline dimensions, experience has shown that D-regions (that is, "disturbed" regions where strain distributions are significantly nonlinear) are vulnerable to premature shear failures near concentrated loads, corners, and supports. Therefore, a "shear protection" algorithm was introduced into the proposed procedure to approximately account for the increased strength of D-regions. This algorithm first detects the joints of frames (beam and column connection nodes), the point load application points, and the supports. It then determines all members that fall within the distance of $0.7 \times h_s$ from such joints, as defined by CSA A23.3-04 Clause 11.3, where h_s is the cross-section depth. Finally, the shear forces acting on those members are reduced, when calculating shear strains, to prevent premature failures. More details of this implementation are provided by Guner (2008).

Shear compatibility strain

A shear compatibility strain γ_{ltc} is calculated for each member as defined by

$$\gamma_{ltc} = \gamma_{ltc}^{pre} + 1.15 \times \frac{V_{UN}}{G_c \times A_t} \tag{1}$$

In Eq. (1), γ_{ltc} is the shear compatibility strain to be used in the current global frame analysis iteration, γ_{ltc}^{pre} is the shear compatibility strain of the previous global frame analysis iteration, V_{UN} is the unbalanced shear force, G_c is the elastic shear modulus as defined by Eq. (2), and A_t is the transformed cross-sectional area. A shear area factor of 1.15 is assumed in Eq. (1) for general cross sections.

$$G_c = \frac{E_c}{2 \times (1 + \nu)} \tag{2}$$

In Eq. (2), E_c is the initial tangent modulus of elasticity of concrete, and ν is Poisson's ratio, which is initially assumed to be 0.15.

Compatibility restoring forces

The axial, moment, and shear compatibility restoring forces are determined for each frame member as follows

$$N_R = N_R{}^{pre} + N_{UN} \tag{3}$$

$$M_R = M_R{}^{pre} + M_{UN} \tag{4}$$

$$V_R = \gamma_{ltc} \times \frac{12 \times E_c \times I_t}{L_k^2} \tag{5}$$

In Eq. (3) to (5), $N_R{}^{pre}$ and $M_R{}^{pre}$ are the axial and moment compatibility restoring forces from the previous global

frame analysis iteration, respectively; N_{UN} and M_{UN} are the unbalanced axial force and bending moment, respectively; I_t is the transformed moment of inertia of the cross section; and L_k is the length of the member. The calculated compatibility restoring forces are applied to the relevant members, as shown in Fig. 7. Note that the moment $V_R \times L_k/2$ caused by the shear compatibility restoring force is added to satisfy equilibrium.

Joint displacements, reactions, and member end-actions

A load vector $\{p\}$, consisting of fixed-end forces due to applied mechanical loads and compatibility restoring forces, is assembled. Using the classical stiffness-based finite element formulation, a structural stiffness matrix $[k]$ is created and assembled based on the procedure described by Weaver and Gere (1990). The joint displacements $\{u\}$ are then determined based on Eq. (6). Using the calculated nodal displacements, updated nodal coordinates are determined, and new member lengths and direction cosines are calculated. This update is performed to consider geometric nonlinearity. Support reactions and member end-actions relative to the elemental axes are finally calculated.

$$\{u\} = [k]^{-1} \times \{p\} \tag{6}$$

Fixed-end forces due to dowel resistance

The dowel resistance provided by the reinforcing bars may be significant in some cases, for example, in beams or columns with low percentages of shear reinforcement. Dowel action is taken into account for each member through the introduction of resisting fixed-end moments. The dowel force is calculated by taking the stiffness portion of the dowel force-dowel displacement formulation proposed by He and Kwan (2001). Details of this implementation are described in Guner (2008).

End factors and average member forces

End factors are used to average the end actions of members to determine one average axial force, shear force, and bending moment value for each member. To account for a possible concentration of deformations at one particular end, the end with higher actions is typically given a higher weighting in this averaging process. Consequently, the end factors for axial force and bending moment, initially taken as 0.5 for both ends, is gradually changed to 0.75 and 0.25, depending on the acting compressive strain. For cracked members, the end factors for bending moment and axial force are always set to 0.75 and 0.25. For averaging the shear force, end factors of 0.5 are used for all members.

Unbalanced forces

Unbalanced forces are the differences between member forces calculated by the global frame analysis and those obtained from the nonlinear sectional analysis, as follows

$$N_{UN\,k} = N_k - N_{\sec\,k} \tag{7}$$

$$M_{UN\,k} = M_k - M_{\sec\,k} \tag{8}$$

$$V_{UN\,k} = V_k - V_{\sec\,k} \tag{9}$$

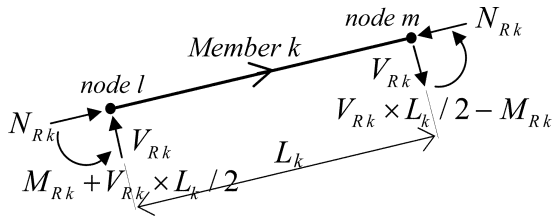

Fig. 7—Compatibility restoring forces in member-oriented axes.

Convergence factors

Convergence factors are needed at the end of each global frame analysis to determine the validity of the analysis results and whether to move on to the next load or time stage. The default criterion is based on the weighted displacements. Details of the formulation can be found in Guner (2008).

Ruptured reinforcement

All reinforcement strains are checked with their rupture strains to determine bar fractures. If a bar fracture is encountered, the stress in that bar is taken as zero for all subsequent load stages.

Shear failure check

In the analyses of shear-critical structures with significant flexural influences, it may occur that, after the shear capacity of one of the members is reached, significant unbalanced shear forces remain present at the end of each load stage instead of ideally being zero. This phenomenon is closely related to the maximum number of global frame analysis iterations permitted because the specified convergence is not usually achieved before the maximum number of iterations is reached in such situations. To deal with this anomaly, a "shear failure check" was introduced into the analytical procedure proposed. If there exists an unbalanced shear force on a member greater than a certain percentage of the acting shear force at the end of more than one load stage, that member is intentionally failed by reducing its moment of inertia to zero. The frame, however, may still continue to carry load based on the conditions of the other members. This percentage was conservatively selected to be 25% based on a parametric study. Other values can also be used because the increasing unbalanced shear force will reach the specified percentage within a limited number of load stages. This check was introduced to provide conservative estimates of the post-peak ductilities of shear-critical structures. More details of this implementation are provided by Guner (2008).

NONLINEAR SECTIONAL ANALYSES

Sectional analyses are performed to determine the nonlinear response of each cross section to imposed sectional deformations. Using a layered (fiber) analysis technique, each concrete and steel layer is analyzed individually based on the disturbed stress field model (DSFM) (Vecchio 2000), although sectional compatibility and sectional equilibrium conditions are satisfied as a whole. The main sectional compatibility requirement enforced is that "plane sections remain plane," which permits the calculation of the longitudinal strain in each layer of concrete, reinforcing, and prestressing steel layer as a function of the top and bottom fiber strains, as shown in Fig. 8. Based on this assumption, the axial strains at the middepths of the members are calculated as defined in Eq. (10). The curvatures of the members are

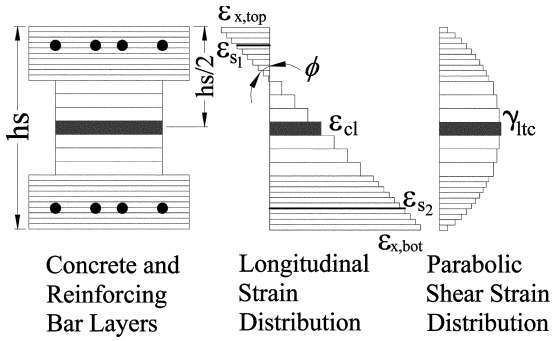

Fig. 8—Longitudinal and shear strain distribution across cross section depth h_s.

calculated from the two end rotations, φ_l and φ_m, and the updated member lengths L_k as defined by Eq. (11).

$$\varepsilon_{cl} = \frac{L_k - L_k^{pre}}{L_k^{pre}} \tag{10}$$

$$\phi = \frac{\varphi_m - \varphi_l}{L_k} \tag{11}$$

$$\varepsilon_{x,top} = \varepsilon_{cl} - \frac{h_s}{2} \times \phi \tag{12}$$

$$\varepsilon_{x,bot} = \varepsilon_{cl} + \frac{h_s}{2} \times \phi \tag{13}$$

It is further assumed that the longitudinal strains in each layer are uniform and equal to the strains at the center of the layer, as shown in Fig. 8. The sectional equilibrium requirements include balancing the axial force, shear force, and bending moment that are calculated by the global frame analysis.

The clamping stresses in the transverse direction are assumed to be zero in the sectional calculations. It is known, however, that high transverse stresses are present at locations where the load is introduced or where a support is present. These stresses locally increase the strength of the member, thereby requiring sectional analyses to be performed at a distance away from the load or support, otherwise producing overly conservative predictions. In the analytical procedure proposed, this phenomenon is approximately accounted for by the "shear protection algorithm," as described previously.

As for the consideration of shear, there are two different approaches available: shear-stress-based analyses based on a uniform shear flow distribution, and shear-strain-based analyses based on either a uniform or parabolic shear strain distribution. By default, the shear-strain-based analysis with parabolic distribution, as shown in Fig. 8, is selected due to its ability to continue an analysis into the post-peak regime (essential for ductility predictions) and its fast and numerically stable execution. This is the approach adopted in the formulations to follow; refer to Guner (2008) for descriptions of the other approaches.

Calculation of longitudinal reinforcement ratios for sectional calculations

In the application of the DSFM to the sectional analyses, smeared reinforcement ratios must be defined for each concrete layer to form the composite material stiffness matrix; therefore, the longitudinal reinforcing or prestressing bar layers defined for each cross section must be smeared to concrete layers. For this purpose, the bar layers are assumed to be smeared in a tributary area of 7.5 times the bar diameters on both sides of the bars, as suggested by CEB-FIP (1990). The resulting reinforcement ratio is used in the sectional analyses when analyzing the related concrete layer.

Average crack spacings

A reasonable estimate of the average crack spacing is needed for crack slip calculations. In the analytical procedure proposed, a variable crack spacing formulation is adapted from Collins and Mitchell (1991). In contrast to the constant crack spacing, the variable crack spacing model considers the fact that the crack spacing becomes larger as the distance from the reinforcement increases. As a result, each concrete layer may have different crack spacings in the longitudinal and transverse directions based on the reinforcement quantity and configuration. Calculation details of this implementation are found in Guner (2008).

Shear-strain-based layer analysis

The purpose of the shear-strain-based layer analysis is to calculate the longitudinal stress σ_x and shear stress τ_{xy} of each concrete layer.

Consider a single concrete layer that has a certain percentage of longitudinal and transverse reinforcement (for example, Fig. 8, shaded layer). To calculate the principal strains in this layer, ε_y must be determined; ε_x and γ_{xy} are known from the global analysis. Any value can be assumed for ε_y to start the iterative calculation process. The net principal strains, ε_{c1} and ε_{c2}, and the orientation of stress field θ can be calculated from a Mohr's circle of strain. The corresponding principal stresses, f_{c1} and f_{c2}, are calculated based on the constitutive relationships of the DSFM.

The concrete material secant moduli are then calculated based on Fig. 9(a) as follows

$$\overline{E}_{c1} = \frac{f_{c1}}{\varepsilon_{c1}} \tag{14}$$

$$\overline{E}_{c2} = \frac{f_{c2}}{\varepsilon_{c2}} \tag{15}$$

$$\overline{G}_c = \frac{\overline{E}_{c1} \times \overline{E}_{c2}}{\overline{E}_{c1} + \overline{E}_{c2}} \tag{16}$$

In Fig. 9(a), ε_c is the concrete net strain (that is, the strain that causes stress); $\varepsilon_c^{\,o}$ is the concrete elastic offset strain due to lateral expansion, thermal, shrinkage and prestrain effects; $\varepsilon_c^{\,p}$ is the concrete plastic offset strain due to cyclic loading and damage; and $\varepsilon_c^{\,s}$ is the concrete crack slip offset strain due to shear slip.

As the DSFM considers reinforced concrete as an orthotropic material in the principal stress directions, it is necessary to formulate the concrete material stiffness matrix $[D_c]'$ relative to those directions as follows

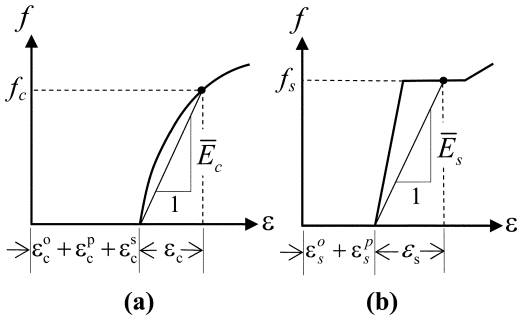

(a) **(b)**

Fig. 9—Determination of secant moduli: (a) concrete; and (b) reinforcement.

$$[D_c]' = \begin{bmatrix} \overline{E}_{c1} & 0 & 0 \\ 0 & \overline{E}_{c2} & 0 \\ 0 & 0 & \overline{G}_c \end{bmatrix} \tag{17}$$

The concrete material stiffness matrix can then be transformed to the global axes as follows

$$[T_c] = \begin{bmatrix} \cos^2\theta & \sin^2\theta & \cos\theta\sin\theta \\ \sin^2\theta & \cos^2\theta & -\cos\theta\sin\theta \\ -2\cos\theta\sin\theta & 2\cos\theta\sin\theta & \cos^2\theta - \sin^2\theta \end{bmatrix} \tag{18}$$

$$[D_c] = [T_c]^T \times [D_c]' \times [T_c] \tag{19}$$

Reinforcement secant moduli are calculated based on Fig. 9(b) as follows

$$\overline{E}_{sx} = \frac{f_{sx}}{\varepsilon_{sx}} \tag{20}$$

$$\overline{E}_{sy} = \frac{f_{sy}}{\varepsilon_{sy}} \tag{21}$$

In Fig. 9(b), ε_s is the reinforcement net strain (that is, the strain that causes stress); ε_s^o is the reinforcement elastic offset strain due to thermal and prestrain effects; ε_s^p is the reinforcement plastic offset strain due to cyclic loading and yielding; and f_s is the reinforcement stress calculated by Eq. (35) to (38).

Because the reinforcement components lie in two orthogonal directions, the global x and y axes, the reinforcement stiffness matrix becomes as shown as follows

$$[D_s] = \begin{bmatrix} \rho_x \times \overline{E}_{sx} & 0 & 0 \\ 0 & \rho_y \times \overline{E}_{sy} & 0 \\ 0 & 0 & 0 \end{bmatrix} \tag{22}$$

The resulting composite material stiffness matrix is calculated as

$$[D] = [D_c] + [D_s] \tag{23}$$

The layer stresses can then be found as

$$[\sigma] = [D] \times [\varepsilon] - [\sigma^o] \tag{24}$$

In Eq. (24), both the [D] matrix and the [ε] vector are based on total strains, necessitating the deduction of [σ^o], a pseudo stress matrix arising from the strain offsets shown in Fig. 9.

$$[\sigma^o] = [\sigma_c^o] + \sum_{r=1}^{2} [\sigma_s^o]_r = \begin{bmatrix} S_{01} \\ S_{02} \\ S_{03} \end{bmatrix} \tag{25}$$

$$[\sigma_c^o] = [D_c] \times ([\varepsilon_c^o] + [\varepsilon_c^p] + [\varepsilon_c^s]) = [D_c] \times \left(\begin{bmatrix} \varepsilon_{cx}^o \\ \varepsilon_{cy}^o \\ \gamma_{cxy}^o \end{bmatrix} + \begin{bmatrix} \varepsilon_{cx}^p \\ \varepsilon_{cy}^p \\ \gamma_{cxy}^p \end{bmatrix} + \begin{bmatrix} \varepsilon_{cx}^s \\ \varepsilon_{cy}^s \\ \gamma_{cxy}^s \end{bmatrix} \right) \tag{26}$$

$$\sum_{r=1}^{2} [\sigma_s^o]_r = \sum_{r=1}^{2} [D_s] \times ([\varepsilon_s^o] + [\varepsilon_s^p])_r = [D_s] \times \begin{bmatrix} \varepsilon_{sx}^o + \varepsilon_{sx}^p \\ 0 \\ 0 \end{bmatrix} + [D_s] \times \begin{bmatrix} 0 \\ \varepsilon_{sy}^o + \varepsilon_{sy}^p \\ 0 \end{bmatrix} \tag{27}$$

The layer stresses can then be calculated as follows

$$\begin{bmatrix} \sigma_x \\ \sigma_y \\ \tau_{xy} \end{bmatrix} = \begin{bmatrix} D_{11} & D_{12} & D_{13} \\ D_{21} & D_{22} & D_{23} \\ D_{31} & D_{32} & D_{33} \end{bmatrix} \times \begin{bmatrix} \varepsilon_x \\ \varepsilon_y \\ \gamma_{xy} \end{bmatrix} - \begin{bmatrix} S_{01} \\ S_{02} \\ S_{03} \end{bmatrix} \tag{28}$$

Taking advantage of the assumption that there is no clamping stress in the transverse direction, Eq. (28) can be expanded as

$$\sigma_y = D_{21} \times \varepsilon_x + D_{22} \times \varepsilon_y + D_{23} \times \gamma_{xy} - S_{02} = 0 \tag{29}$$

This assumption permits the calculation of the total strain in the transverse direction, which is the basic unknown of the procedure.

$$\varepsilon_y = \frac{-D_{21} \times \varepsilon_x - D_{23} \times \gamma_{xy} + S_{02}}{D_{22}} \tag{30}$$

Using the calculated ε_y value, the new principal stresses (f_{c1} and f_{c2}) are determined from the corresponding principal strains (ε_{c1} and ε_{c2}) using the DSFM constitutive models; the aforementioned calculations are repeated until the ε_y value converges or the specified maximum number of iterations is reached (100 iterations by default). At the conclusion of these calculations, the required stress values are calculated as follows

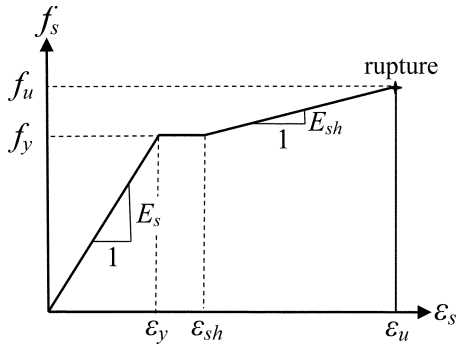

Fig. 10—Trilinear stress-strain relationship for reinforcement.

$$\sigma_x = D_{11} \times \varepsilon_x + D_{12} \times \varepsilon_y + D_{13} \times \gamma_{xy} - S_{01} \quad (31)$$

$$\tau_{xy} = D_{31} \times \varepsilon_x + D_{32} \times \varepsilon_y + D_{33} \times \gamma_{xy} - S_{03} \quad (32)$$

Reinforcement response

The reinforcement response must be superimposed on the concrete response to obtain the resultant nonlinear sectional forces, which require the determination of net reinforcement strains. In the most general case, the total longitudinal reinforcement strain ε_{sj} is composed of net strain ε_j^{net} (that is, the strain that causes stress), prestrain offset strains $\Delta\varepsilon_{pj}$ due to prestressing, elastic offset strains ε_{sj}^{th} due to thermal effects, and plastic offset strains ε_{sj}^{p} due to cyclic loading and yielding. The resulting strain becomes

$$\varepsilon_{sj} = \varepsilon_j^{net} - \Delta\varepsilon_{pj} + \varepsilon_{sj}^{th} + \varepsilon_{sj}^{p} \quad (33)$$

The total strain ε_{sj} for each reinforcing or prestressing steel layer is determined from the longitudinal strain distribution given in Fig. 8. In this calculation, the strain values corresponding to the center of the bar are considered.

As for the transverse reinforcement, the total strain ε_{yi} is similarly decomposed into its components except that no prestrains are considered, as defined as follows

$$\varepsilon_{yi} = \varepsilon_{yi}^{net} + \varepsilon_{yi}^{th} + \varepsilon_{yi}^{p} \quad (34)$$

In Eq. (34), subscript *i* refers to the concrete layer number as the transverse reinforcement is smeared into concrete layers.

After determining the net strains for the reinforcement components, the reinforcement responses, whether in the longitudinal (x) or transverse (y) directions in compression or in tension, is calculated by a trilinear relationship as shown in Fig. 10, with corresponding stresses defined as follows

$$f_s = E_s \times \varepsilon_s \quad \text{for } 0 \le \varepsilon_s < \varepsilon_y \quad (35)$$

$$f_s = f_y \quad \text{for } \varepsilon_y \le \varepsilon_s \le \varepsilon_{sh} \quad (36)$$

$$f_s = f_y + E_{sh} \times (\varepsilon_s - \varepsilon_{sh}) \quad \text{for } \varepsilon_{sh} < \varepsilon_s < \varepsilon_u \quad (37)$$

$$f_s = 0 \quad \text{for } \varepsilon_s \ge \varepsilon_u \quad (38)$$

In Eq. (35) to (38), f_s is the stress, f_y is the yield stress, f_u is the ultimate stress, ε_s is the net strain, ε_y is the yield strain, ε_{sh} is the strain at the onset of strain hardening, and ε_u is the ultimate strain of the reinforcement.

Local crack calculations

The consideration of local crack conditions is an essential component of the procedure. These calculations are performed to make sure that the average concrete stresses can be transmitted across cracks by the reserve capacity of the reinforcement. In addition, the shear stresses v_{ci} developed at the crack interface are calculated for each concrete layer to determine the magnitude of the shear slip along the crack surfaces. The local crack calculations are performed within each sectional analysis iteration for each concrete layer using the formulations of the DSFM as described by Vecchio (2000). A detailed description of the adaptation into the frame analysis algorithm is provided by Guner (2008).

Resultant sectional member forces

After determining both the concrete and reinforcement responses, the resultant sectional forces are obtained by superposition as shown below, where *ncl* is the total number of concrete layers and *nsl* is the total number of reinforcing and prestressing steel layers.

$$N_{sec\,k} = \sum_{i=1}^{ncl} \sigma_{xi} \times b_i \times h_i + \sum_{j=1}^{nsl} f_{sxj} \times A_{sj} \quad (39)$$

$$M_{sec\,k} = \sum_{i=1}^{ncl} \sigma_{xi} \times b_i \times h_i \times y_{ci} + \sum_{j=1}^{nsl} f_{sxj} \times A_{sj} \times y_{sj} \quad (40)$$

$$V_{sec\,k} = \sum_{i=1}^{ncl} \tau_{xy} \times b_i \times h_i \quad (41)$$

The calculated forces are returned to the global frame analysis algorithm, where they are checked with the member forces obtained from the global frame analysis to determine the unbalanced forces. The objective of the global frame analysis is to reduce all unbalanced forces to zero before proceeding to a new load or time stage.

ADDITIONAL CONSIDERATIONS

Concrete dilatation (Poisson's effect)

Under biaxial stress conditions, it is common to assume that Poisson's effects are negligible for cracked concrete. If the concrete is uncracked or if the tensile straining in the cracked concrete is relatively small, however, the lateral expansion of concrete due to Poisson's effects can account for a significant portion of the total strains, requiring these effects to be taken into account. Due to internal micro-cracking, Poisson's ratio increases as the acting compressive stress increases, causing concrete expansion to accelerate. When confined by transverse or out-of-plane reinforcement, the lateral expansion results in passive confining stresses that considerably improve the strength and ductility of the reinforced concrete under compression. This phenomenon is taken into account in the sectional analyses of the proposed procedure as concrete elastic offset strains ε_c^{o} based on the lateral expansion model of Kupfer et al. (1969). Details of these calculations are provided by Guner (2008).

Concrete prestrains

Concrete prestrains, such as shrinkage strains ε_{sh}, are also considered as a loading and can be assigned to desired

members. These prestrains are treated as elastic concrete offsets (that is, $\varepsilon_{cx}^{o} = \varepsilon_{sh}$ and $\varepsilon_{cy}^{o} = \varepsilon_{sh}$, while $\gamma_{cxy}^{o} = 0$) and are included in the sectional analyses.

Out-of-plane (confinement) reinforcement

Lateral expansion causes passive confining pressures in the transverse and out-of-plane reinforcement, which may considerably improve the strength and ductility of the concrete. In the analytical procedure proposed, the stress in the transverse reinforcement due to lateral expansion is inherently taken into account by the use of concrete elastic offset strains, as formulated previously. Stresses in the out-of-plane reinforcement are calculated separately in the sectional analyses. The calculated confining stress is taken into account to enhance the concrete compressive response, as described in Guner (2008).

SUMMARY AND CONCLUSIONS

Although modern design codes typically require reinforced concrete frames to be designed for ductile and flexure-critical behavior, situations often arise in practice where shear-related mechanisms play a significant role in structural response. Omission of shear effects for such structures typically results in severely unconservative and unsafe calculation of strength and ductility. Most available tools, however, either ignore shear mechanisms altogether, employ unclear or overly simplistic formulations, or require complex precalculation of shear hinge properties using separate software, as well as selection of numerous analysis options and parameter values.

A computer-based analytical procedure, VecTor5, has been developed for the nonlinear analysis of frame-related structures consisting of beams, columns, and shear walls, under monotonic and pushover loads. Based on the disturbed stress field model (DSFM), the procedure is capable of capturing shear-related effects coupled with flexural and axial behaviors. The proposed procedure is based on two interrelated analyses, using an iterative total load, secant stiffness formulation. A classical stiffness-based linear-elastic frame analysis is performed as the main framework of the procedure. Rigorous sectional analyses of concrete member cross sections are then undertaken, using a distributed-nonlinearity fiber model and the constitutive relations of the DSFM. The computed responses are then enforced with the use of an unbalanced force approach, where the unbalanced forces are reduced to zero in an iterative process. The procedure allows for the analysis of frames with unusual or complex cross sections under a large range of static and thermal load conditions. The formulations presented herein can be incorporated into most linear-elastic frame analysis procedures.

The procedure is capable of considering significant second-order effects such as material and geometric nonlinearities, time- and temperature-related effects, membrane action, nonlinear degradation of concrete and reinforcement at elevated temperatures, concrete compression softening, tension stiffening and tension softening, shear slip along crack surfaces, nonlinear concrete expansion, confinement effects, previous loading history, effects of slip distortions on element compatibility relations, concrete prestrains, and reinforcement dowel action. Furthermore, new or improved formulations can be adopted as they become available. Currently, however, the procedure does not account for reinforcement bond slip and compression bar buckling mechanisms. Furthermore, as is typical in frame analysis of this type, the procedure uses centerline dimensions of cross sections together with stiffened joint panel zone members. Therefore, failure modes involving beam-column panel zones cannot be captured. A nonlinear member type should be developed for beam-column joints to further improve the capabilities of the proposed procedure. Future work will be directed toward addressing these limitations.

The advantage of the proposed method over others is its inherent and accurate consideration of shear-related mechanisms within a simple modeling process suitable for practical applications. Unlike other methods, decisions regarding the expected behavior and failure mode, or selection of appropriate analysis options and parameter values, are not required in the modeling process prior to the analysis, nor are additional calculations, such as the moment-axial force, moment-curvature, or shear force-shear deformation responses of the cross sections. Furthermore, the procedure exhibits excellent convergence and numerical stability characteristics, requiring little computational time, as demonstrated in a companion paper (Guner and Vecchio 2010) through verification and application studies.

REFERENCES

Carr, A. J., 2005, "User Manual for the 2-Dimensional Version Ruaumoko2D," Department of Civil Engineering, Computer Program Library, University of Canterbury, Christchurch, New Zealand, 87 pp.

CEB-FIP, 1990, "Model Code for Concrete Structures," Design Code, Comité EURO-International du Béton, 437 pp.

Collins, M. P., and Mitchell, D., 1991, *Prestressed Concrete Structures*, Response Publications, Canada, 766 pp.

CSA A23.3, 2004, *Design of Concrete Structures*, Canadian Standards Association, Mississauga, ON, Canada, 214 pp.

CSI, 2005, "Analysis Reference Manual for SAP2000®, ETABS®, and SAFE™," Computers and Structures, Inc., Berkeley, CA, 415 pp.

Duong, K. V.; Sheikh, S. A.; and Vecchio, F. J., 2007, "Seismic Behaviour of Shear-Critical Reinforced Concrete Frame: Experimental Investigation," *ACI Structural Journal*, V. 104, No. 3, May-June, pp. 304-313.

FEMA 356, 2000, "Prestandard and Commentary for the Seismic Rehabilitation of Buildings," Federal Emergency Management Agency, Nov., Washington, DC, 518 pp.

Guner, S., 2008, "Performance Assessment of Shear-Critical Reinforced Concrete Plane Frames," PhD thesis, Department of Civil Engineering, University of Toronto, Toronto, ON, Canada, 429 pp. (http://www.civ.utoronto.ca/vector/) (accessed Oct. 10, 2009).

Guner, S., and Vecchio, F. J., 2008, "User's Manual of VecTor5," (http://www.civ.utoronto.ca/vector/) (accessed Oct. 10, 2009).

Guner, S., and Vecchio, F. J., 2010, "Pushover Analysis of Shear-Critical Frames: Verification and Application," *ACI Structural Journal*, V. 107, No. 1, Jan-Feb., pp. 72-81.

He, X. G., and Kwan, A. K. H., 2001, "Modeling Dowel Action of Reinforcement Bars for Finite Element Analysis of Concrete Structures," *Computers and Structures*, V. 79, No. 6, pp. 595-604.

IBC, 2006, "International Building Code," International Building Code Council, 679 pp.

Kupfer, H.; Hilsdorf, H. K.; and Rusch, H., 1969, "Behavior of Concrete under Biaxial Stress," ACI JOURNAL, *Proceedings* V. 66, No. 8, Aug., pp. 656-666.

Prakash, V.; Powell, G. H.; and Campbell, S. D., 1993, "Drain-2DX Base Program Description and User Guide: Version 1.10," UCB/SEMM-1993/17, Department of Civil Engineering, University of California, Berkeley, CA, 97 pp.

Vecchio, F. J., 1987, "Nonlinear Analysis of Reinforced Concrete Frames Subjected to Thermal and Mechanical Loads," *ACI Structural Journal*, V. 84, No. 6, Nov.-Dec., pp. 492-501.

Vecchio, F. J., 2000, "Disturbed Stress Field Model for Reinforced Concrete: Formulation," *Journal of Structural Engineering*, ASCE, V. 126, No. 9, pp. 1070-1077.

Vecchio, F. J., and Collins, M. P., 1988, "Predicting the Response of Reinforced Concrete Beams Subjected to Shear Using Modified Compression Field Theory," *ACI Structural Journal*, V. 85, No. 3, May-June, pp. 258-268.

Weaver, W., and Gere, J. M., 1990, *Matrix Analysis of Framed Structures*, third edition, Van Nostrand Reinhold, New York, 546 pp.